NUMERICAL SIMULATION OF FLOW AROUND A CURVED CYLINDER WITH VARYING DIAMETER.

NTNU

EMIL SEVERIN MOEN RAMSVIK (ESRAMSVI@STUD.NTNU.NO)
SUPERVISOR: PROFESSOR BJØRNAR PETTERSEN
CO-SUPERVISOR: POST.DOC FENGJIAN JIANG

Problem

In marine hydrodynamics, the need for accurate numerical simulations of viscous fluid flow around geometrical configurations modeling subsea pipelines and risers have arisen. Using a Direct Numerical Solution technique (DNS) to fully resolve the Navier-Stokes equation can provide an accurate benchmark for further studies.

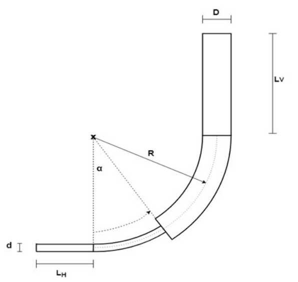

Figure 1: Set up of geometry. α is the angle were the change in diameter occurs.

Introduction

Pipelines and risers often experience dynamic fluid phenomena such as Vortex Induced Vibrations (VIV). It has been know for some time that buoyancy elements can suppress VIV [1]. By applying Computational Fluid Dynamics (CFD) solvers, flow around geometrical configurations can be investigated in detail.

This thesis investigates how geometrical features such as changes in diameter and curvature affect the wake and flow phenomenon using numerical analysis.

Numerical Solver

MGLET [1] is developed for numerical simulation of turbulent flow around complex geometries. It uses a number of techniques to save CPU and memory. It runs efficiently on a parallel computer with up to 2000 processors. MGLET is based on a finite volume formulation of the Navier-Stokes equations. It models the body using an Immersed Boundary Method on a Cartesian grid [2]

[1]MGLET stands for Multi-Grid Large Eddy Turbulence and is a numerical Navier-Stokes solver for both Large Eddy Simulation and DNS.

Results

Two simulations where a change in diameter D/d = 5, at α = 90º i.e. from the start of the vertical extension were investigated. Strong axial flow was induced from the curvature. The step creates an upwash/downwash towards the large diameter cylinder. The introduction of a step can either increase or counteract the axial flow from the curvature, depending on the configuration.

Frequency analysis identified 4 regions of interest in the wake of the concave cylinder with a change in diameter at α = 90º (Figure 2). The curved cylinder part sheds vortices with a Strouhal frequency of $St_d = \frac{fU_0}{d} = 0.114$ and the vertical extension has a Strouhal frequency of $St_D = \frac{fU_0}{D} = 0.2$ (Figure 3).

The parameter study showed that geometrical configurations could be divided into 3 groups. The first group contains changes in diameter at α <= 45º. It is categorized by recirculation zones in front of and behind the step. The strong helical vortices are formed behind the recirculation zones.

The second group contains the cases with 45º<= α < 70º. This group has unique behaviour not seen in other cases. For α = 60º, vortex structures similar to those shed from the small cylinder is shed from the step.

The last group contains all cases with α >= 70º. This group have no recirculation zones, but for high α values vortex shedding is observed behind the small curved cylinder. The vortex shedding from the small cylinder is forced upwards by both the curvature and the step creating an area of the wake with mixed vortex shedding.

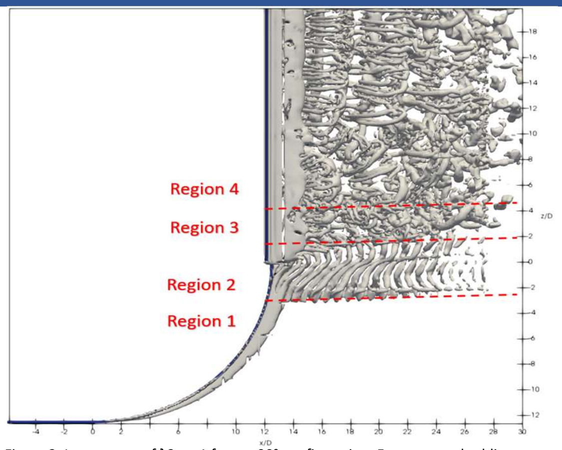

Figure 2: Iso-contour of λ2 = - 1 for α = 90° configuration. Four vortex shedding regions were identified. Region 1 has a helical vortex following the cylinder, Region 2 sheds vortices from the small cylinder. Region 3 has a mix of vortex structures from Region 2 and 4. Region 4 experiences regular von Karman vortex shedding.

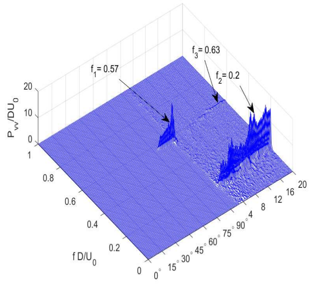

Figure 3: Power density spectrum of the cross flow velcoity v, for α = 90°. The elocity was sampled at a distance of 3D behind the cylinder in the y/D = 0 plane. The peaks indicates at what frequencies the vortices shed. The arrows indicates frequencies of interest.

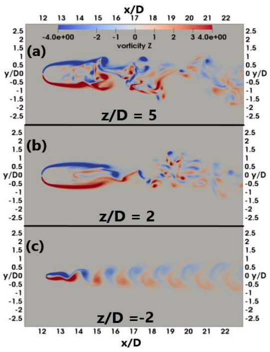

Figure 4: Contour plot of the vorticity ωz for α = 90°. (a) shows the vorticity in Region 4, (b) shows Region 3 and (c) in Region 2.

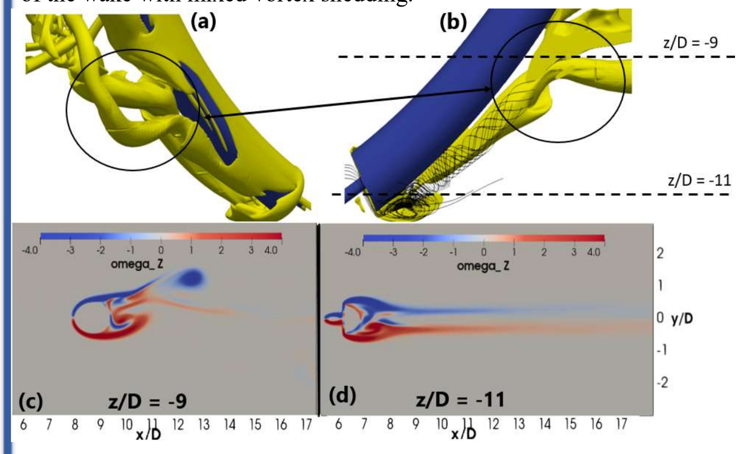

Figure 5: (a) Iso-contour of λ2 = -1, as seen behind the cylinder. (b) Iso-surface of λ2 = -1 and streamlines of the velocity at recirculation zones and vortex structures. (c) Instantaneous z-dir. vorticity ωz contour plot in a (x,y)-plane at z/D = -9, i.e. were the helical vortex dislocates. (d) Same as (c) but at z/D =-11, i.e. just above the step bottom edge.

Of special interest was the α = 30º case, which had vortex structures unique to this case. In the immediate wake of the step, a recirculation bubble was formed and a helical vortex is also formed behind it (Figure 5 (b)). The helical vortex dislocates from the cylinder at z/D = -9 as indicated in Figure 5. This dislocation of the helical vortex so close to its formation was only evident in the α = 30º case. The vorticity plot in Figure 5 (c) shows the helical vortex structure close to the cylinder surface and the dislocated vortex at x/D = 12.5. The recirculation bubble is just below the bottom edge of the step (Figure 5 (b)), and has a oval shape which differs from other cases.

References

[1] Vandiver, J., Peoples, W, W., 01 2003. The effect of staggered buoyancy modules on flow-induced vibration of marine risers.

[2] Peller, N., Le-Duc, A., Tremblay, F., Manhart, M., 2006. High-order stable interpolations for immersed boundary methods. International journal for numerical methods in fluids54, 1175.1193

Acknowledgements

The author would like to thank supervisors professor Bjørnar Pettersen and Post.Doc Fengjian Jiang. The author also thank for Phd. Cai Tian for valuable input and comments. The work also received support from the Research Council of Norway (Program for Supercomputing, under project: NN9191K) through a grant of computing time.

Conclusions

The parameter study showed that the fluid flow follow a pattern with the angle of the step. At low step-angles α, recirculation zones appear around the step. At angles higher than 45º, the recirculation zones disappear and the vortex shedding from the small cylinder starts to occur at very high angles (α > 75º).